Available online at www.sciencedirect.com
SCIENCE DIRECT
Polymer 46 (2005) 7463–7472
polymer
www.elsevier.com/locate/polymer

# On the role of inter- and intra-molecular potentials in the simulation of vitrification with the bond fluctuation model

J. Molina-Mateo[a,*], J.M. Meseguer-Dueñas[a], J.L. Gómez-Ribelles[b]

[a]*Department of Applied Physics, Center for Biomaterials, Universidad Politécnica de Valencia, Camino de Vera s/n, E-46071 Valencia, Spain*
[b]*Department of Applied Thermodynamics, Center for Biomaterials, Universidad Politécnica de Valencia, Camino de Vera s/n, E-46071 Valencia, Spain*

Received 11 May 2005; received in revised form 7 June 2005; accepted 12 June 2005
Available online 7 July 2005

**Abstract**

The glass transition of linear chain polymers was simulated by means of the bond fluctuation model, employing a Lennard–Jones intermolecular potential and a bond-length intra-molecular potential. The influence of the balance between inter- and intra-molecular potentials on the model prediction was studied and an appropriate range was determined in order to simulate physical ageing. The relationship between molecular mobility and the dynamically accessible volume was shown in comparison with other definitions of specific volume or free volume. The temperature dependence of the dynamically accessible volume shows the vitrification of the material analogously to the temperature dependence of the lattice energy. Dynamically accessible volume has been proposed as a universal parameter to explain glass transition, but in the bond fluctuation model it does not give the same value for all simulated glass transitions. This fact could be corrected by including the Metropolis criterion in the dynamically accessible volume in order to extend the concept to thermal systems.


*Keywords:* Bond fluctuation model; Dynamically accessible volume; Glass transition

## 1. Introduction

Vitrification is still one of the unsolved problems in physics. A liquid vitrifies, or becomes glass, when its viscosity reaches very high values, typically higher than $10^{12}$ P, in a process that prevents the formation of the crystalline structure. The viscosity is then high enough to ensure the lack of the molecular mobility necessary for the molecules to attain the probably existing crystal germs and to start crystal growing. Several processes have been proposed to vitrify substances of low molecular weight. For instance, a process based on spraying the liquid onto a super-cooled metal plate has demonstrated the possibility of vitrifying water [1]. In this case the extremely high cooling rate simply leaves no time for the molecules to reorganize in the temperature interval in which the crystallization kinetics would allow it. Then, on cooling, molecular mobility is reduced exponentially with decreasing temperature, and around 140 K glass transition takes place and water becomes glass.

For a given thermal history, the ability of a substance to vitrify depends on several factors; one of them is obviously its chemical regularity, which should make the molecules capable of fitting into a tridimensional lattice. Atactic polymers are the best model of glass-formers since they cannot form a regular crystal, thus they always vitrify on cooling. But there is a wide variety of regularity ranges, starting with the simplest low-molecular liquids such as argon at one extreme and the atactic polymers at the other. Another important factor is the association of the molecules through hydrogen bonding, which has caused some alcohols to be the subject of classic studies on vitrification [2].

One of the characteristics of glass is its lack of long-range order, keeping the molecular organization of a liquid, but the other great difference with the solid is that glass is not in thermodynamic equilibrium. Thus, when glass is formed by a given thermal history, if it is kept in an environment whose thermodynamic conditions remain constant, the glass undergoes a continuous process, called structural relaxation or physical ageing, that tends to reach a state of equilibrium compatible with the conditions of the

* Corresponding author. Tel.: +34 963 877007x75284; fax: +34 963 879 896.
*E-mail address:* jmmateo@fis.upv.es (J. Molina-Mateo).

0032-3861/$ - see front matter © 2005 Elsevier Ltd. All rights reserved.
doi:10.1016/j.polymer.2005.06.022

environment. During physical ageing at constant temperature and pressure the free energy of the system continuously diminishes, which implies a continual decrease in volume, enthalpy and entropy with time. The kinetics of physical ageing are a consequence of the residual ability of the molecules to reorganize in the glass state, which obviously is not null. Molecular rearrangement is possible through molecular displacement in the case of substances of low molecular weight, or conformational rearrangement of the chain segments in the case of polymers. One of the problems involved is to understand the physical and chemical factors that govern molecular mobility both above and below glass transition: the role of inter- and intra-molecular interactions, geometrical restrictions of motion, etc. and to determine if there is any critical value of a physical parameter that causes the onset of vitrification or the glass transition process on cooling.

Classical computer simulation approaches can still be used to give an insight into these fundamental aspects. The two main techniques employed are molecular dynamics simulations [3–15] and Monte Carlo calculations [16–24]. The former is based on the solution of the equations of movement of a set of particles, while the Monte Carlo system is based on stochastic calculations of possible configurations of the system. Although both techniques were introduced 50 years ago, their practical application has experienced a development parallel to the evolution of computers. Glass transition and physical ageing can be studied by both approaches [15,17,21,25–31], as both techniques can add to our knowledge of these processes.

The aim of this work is firstly to discuss the role of the inter- and intra-molecular potentials on the structure and mobility of the glass that results from a liquid cooled at a constant rate from equilibrium. Secondly, we will discuss the use of the dynamically accessible volume (see below) as a useful variable to observe glass transition.

## 2. Model hypothesis and simulation routines

The bond fluctuation model [17,32–34] is one of the most widely employed Monte Carlo models for simulating the behaviour of polymers. The model has been applied to the study of the systems of many different materials and to different properties, such as molecular motion [17,32–39], the influence of molecular size [38,40,41], glass transition [17,21,25–31], multicomponent systems [42–44], polymers at interfaces [40,45] and confined polymers [46].

The three-dimensional bond fluctuation model is a lattice model in which a molecular group representing between 3 and 5 carbons of the polymeric chain, occupies eight cells forming a cube. The distance between two bonded molecular groups can fluctuate between 2 and $\sqrt{10}$ units of the lattice, excluding bonds at a distance of $\sqrt{8}$ in order to avoid bond-crossing [33,47]. Two potentials can be included in order to evaluate the potential energy of the system [30]. First a truncated Lennard–Jones potential, calculated up to a distance of four lattice cells, representing inter-molecular interactions:

$$U_{\mathrm{LJ}}(r) = 4\varepsilon\left[\left(\frac{\sigma}{r}\right)^{12} - \left(\frac{\sigma}{r}\right)^{6}\right] \tag{1}$$

and a bond length potential representing intra-molecular interactions:

$$U(l) = U_0(l - l_0)^2 \tag{2}$$

The dynamics of the model consist of proposing a local monomer jump of one lattice unit and either accepting or rejecting it after considering the Metropolis transition probability [33]

$$P = \min\left[1,\ \exp\left(\frac{-\Delta E}{k_{\mathrm{B}}T}\right)\right] \tag{3}$$

which makes temperature play a role in the model simulation.

The effect of including both potentials is that competition appears between them and the behavior of the model depends on the contribution of each one to the total energy. When only one potential is employed, according to one of the Eqs. (1) or (2), usually $\varepsilon$ or $U_0$ (depending on the potential used) is chosen with a value of 1 and the evolution of the system depending on reciprocal temperature (or more frequently on $\beta = 1/k_{\mathrm{B}}T$, $k_{\mathrm{B}}$ being Botzmann's constant) is observed. The model simulation becomes independent of the value chosen for $\varepsilon$ or $U_0$ if the results are expressed in terms of $\beta' = \varepsilon/k_{\mathrm{B}}T$, or $\beta'' = U_0/k_{\mathrm{B}}T$.

When two potentials are employed, the temperature dependence of the material properties must be expressed in terms of $\beta = 1/k_{\mathrm{B}}T$, and no obvious normalization exists. Wittkop et al. [30] proposed using $\varepsilon = U_0$ and expressing the temperature dependence through $\beta''' = (\varepsilon + U_0)/k_{\mathrm{B}}T$. The balance between inter- and intra-molecular potentials can be defined by the balance factor:

$$B_{\mathrm{f}} = \frac{U_0}{\varepsilon} \tag{4}$$

In Ref. [30] $B_{\mathrm{f}} = 1$.

The value of $B_{\mathrm{f}}$ somehow characterizes the influence of inter- and intra-molecular potentials in the molecular organization, but its interpretation is not straightforward. In fact, $B_{\mathrm{f}} = 1$ is far from corresponding to a system where both energies are perfectly balanced, introducing competition between potentials, since the value of $\Delta E$ in Eq. (3) depends not only on the values of $\varepsilon$ or $U_0$ but also on the number of interactions per molecular group, which determines how many times Eqs. (1) and (2) must be evaluated. In an inner molecular group belonging to a polymeric chain Eq. (2) is evaluated twice, while the number of evaluations of Eq. (1) depends on the local density around the molecular group. So it is not easy to ascertain if potentials are really balanced or if one of them is

controlling the behaviour of the whole system, through their respective contributions to $\Delta E$. By means of this Balance Factor we aim to determine which potential predominates in a system with $B_f=1$ and what happens if we simulate systems with different values for $B_f$.

In this work all simulations consisted of a three-dimensional box ($L=40$) occupied by size 10 chains with a density of $\phi=0.5$. The $\sigma$ parameter of the Lennard–Jones potential was chosen as $\sigma=2.0$ in order to represent the volume exclusion of molecular groups, while the bond length potential parameter $l_0$ was 3.0 in order to introduce competition between both potentials. The Lennard–Jones potential was only calculated up to a maximum distance of four lattice units for reasons of computational efficiency.

The thermal history consisted of an equilibrating time of $10^5$ Monte Carlo steps (MCS) at a temperature given by $k_BT=5$. After the initial equilibrium configuration was reached, we applied a cooling ramp that decreased $0.1k_BT$ units per 1000 Monte Carlo Steps. This cooling ramp was followed by an isothermal period at $k_BT=0.1$ for $10^7$ MCS, where the system evolution was observed, and finally a heating ramp was applied observing the same sequence as in the case of the cooling ramp. The evolution of the system was observed throughout the entire process. Special attention was given to the value of the energy of the system, evaluating mean energy per molecular group. Energy values were calculated by averaging the last 5 MCS at every temperature step from 10 statistically independent configurations. In addition, the dynamically accessible volume (see below) was calculated by averaging 10 independent configurations at every temperature step.

In order to observe the structural properties of the system, a spatial pair correlation function [48] was calculated:

$$g(r) = \frac{2L^3H(r)}{(NP)^2h(r)} \tag{5}$$

Where $H(r)$ represents the histogram that counts the number of times an allowed distance $r$ occurs, $h(r)$ corresponds to the number of possible r-vectors for a given distance on the lattice, $L$ is the box simulation size and NP is the total number of particles.

The correlation time function of the center of mass of the chains [17,26,30–35,49–51]

$$g_3(t) = \langle[\vec{r}_{CM}(t) - \vec{r}_{CM}(0)]^2\rangle \tag{6}$$

was also calculated and was used to determine a diffusion coefficient [17,32,34,35,52] defined by:

$$D = \lim_{t\to\infty} \frac{g_3(t)}{6t} \tag{7}$$

All these functions were employed to characterize the influence of the balance factor on the evolution and dynamic properties of the system.

## 3. Results and discussion

### 3.1. Crystallization, glass transition, vitrification on cooling

The results of a computer simulation of a thermal history consisting of a cooling down from $k_BT=5$ to $k_BT=0.1$, an isothermal stage at this temperature and the heating scan from $k_BT=0.1$ to $k_BT=5$ are shown in Fig. 1 in terms of the evolution of the energy throughout the thermal treatment for different values of $B_f$ (Table 1). In the case of the simulations conducted with $B_f=0$ and $B_f=1$ (Fig. 1(a)) a sharp decrease of the energy is shown on cooling, the energy attains its minimum value when $k_BT$ is immediately above the transition, and during the rest of the cooling process this value is kept constant. Any subsequent isothermal annealing in this temperature interval produces no change in the energy of the system. This means that the structure resulting from the transition retains no conformational mobility of the polymer chains. In spite of the connectivity of the monomeric units imposed by the polymeric chain, the

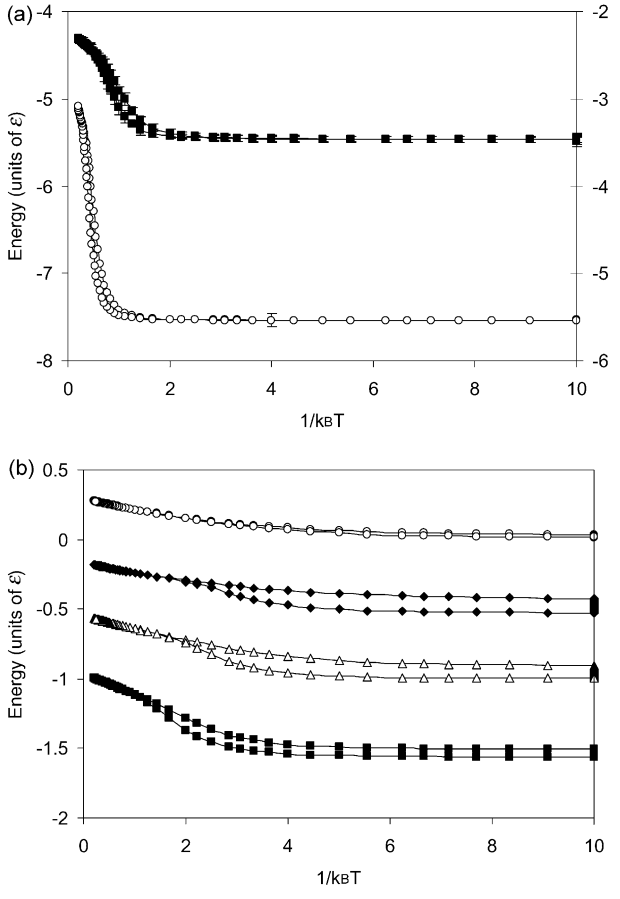


Fig. 1. Temperature dependence of the energy throughout a computer simulated process that starts with a cooling ramp starting from a high temperature equilibrium state includes an isothermal stage at $1/k_BT=10$ followed by a heating ramp. (a) $B_f=0$ (○ in primary axis) and $B_f=1$ (■ in secondary axis); (b) $B_f=3$ (■), $B_f=5$ (△), $B_f=10$ (♦) and $B_f=\infty$ (○). Error bars consisted of ($\pm 3\sigma$) and were sized as dots. Lines are employed only as a guideline for the eye.

Table 1
Chosen values for energy parameters depending on balance factor

| $U_0$ | $\varepsilon$ | $B_f$ |
|---|---|---|
| 0 | 1 | 0 |
| 0.5 | 0.5 | 1 |
| 0.75 | 0.25 | 3 |
| 0.8333 | 0.1666 | 5 |
| 0.9090 | 0.0909 | 10 |
| 1 | 0 | $\infty$ |

attraction potential forces the chains to pack together in a lattice pattern. In the case of $B_f=0$ (only Lennard–Jones potential) no bond potential is considered, thus, there are no preferred orientations in the chain segments and the role of connectivity is not so important. It is interesting to note that the result of the simulation with $B_f=1$ produced similar results. In this respect, the apparent balance between $\varepsilon$ and $U_0$ actually yields a behavior governed by the inter-molecular potential, as Wittkop pointed out [30]. After annealing, both plots show a similar process of hysteresis until the structure of the system again reaches the configuration of a liquid in equilibrium.

At the other extreme, for $B_f=\infty$ (Fig. 1(b)), the transition is gradual, covering a broad $1/k_BT$ interval, and in fact the continuous decrease of the energy is apparent until the lowest temperatures are reached. The decrease of energy during the isothermal stage after cooling is modest but significant, giving conformational mobility at temperatures below the transition. But the clearest results in this aspect are given by the simulations conducted with $B_f$ ranging between 3 and 10. The combination of inter- and intra-molecular potentials in the Bond fluctuation model yields a glass with a mobility that depends on the balance between both types of interaction potentials.

Up to now, there has been no reason to attribute the arrest of mobility and the decrease in energy given by the simulation on cooling to crystallization or vitrification. This will be discussed when we study physical ageing at temperatures below the transition.

The pair-correlation function of all configurations obtained just after transitions at $k_BT=0.1$ (Fig. 2) demonstrates some differences in the intensity of the peaks. The structure attained in the model simulation with low values of $B_f$ is characterized by sharp $g(r)$ peaks appearing at certain distances determined by the lattice geometry. This can be interpreted as representative of the long-range crystalline order. On the other hand, high $B_f$ values decreased the intensity of the $g(r)$ peaks, denoting a more amorphous material. Nevertheless, simulations with $B_f=\infty$ led to $g(r)$ peaks appearing at different characteristic distances than those obtained with low $B_f$ values, due to the preferred distances of bond length potential, indicating a different structure. In order to study the configuration of the polymer chains, we calculated the intra-molecular contribution to the pair-correlation function, using Eq. (5) but taking into account only the pairs of segments pertaining to the same chain ($g_{intra}(r)$). Fig. 3 shows that for low values of $B_f$, when the inter-molecular Lennard–Jones potential dominates the total potential energy of the system, the preferred distance between monomers belonging to the same chain is that corresponding to the vector (2,1,0). As $B_f$ increased, the intensity of the $g(r)$ peak corresponding to this distance diminished, while the intensity corresponding to vector (3,0,0) rose, i.e. the mean distance between bonded monomeric units increased, giving the maximal value for $B_f=\infty$.

### 3.2. Dynamically accessible volume

The definition and calculation of specific volume is a task that has been attempted before with off-lattice models [53] and even with the Bond fluctuation model when volume and density are fixed [30,54,55]. Wittmann [54] proposed an approach to the calculation of the free volume around a monomer for the Bond fluctuation model. Free volume would be related to the number of empty sites in the vicinity of a monomeric unit, which could be occupied in one Monte Carlo Step by a monomer movement subjected to the following conditions:

(i) the volume exclusion must be respected
(ii) the model must allow the bond lengths after the jump
(iii) the jump must be allowed by the Metropolis procedure

Wittkop [30] employed conditions (i) and (ii) with the Bond fluctuation model in order to observe the glass transition, disregarding the Metropolis criterion. According to Ref. [54], condition (ii) is controlled indirectly by the temperature, due to the role that this variable plays in the selection of the preferred bond lengths. Thus, the kinetic and thermodynamic parameters are indirectly taken into account employing the first two conditions. This specific volume is averaged for all monomers and normalized to 1 in order to obtain a value with no dependence on topology.

Independently, Dawson [56–58] has proposed the concept of dynamically accessible volume (DAV) in order to introduce a parameter, which governs the dynamics of dense systems. This concept emphasizes the difference between two kinds of empty cells; those, which can be accessible for a monomer in a single move according to Monte Carlo dynamics, are called holes; the rest of the empty cells are called vacancies. The DAV takes into account holes averaged over the total number of cells in the system in order to obtain a parameter, which expresses the mobility of the system, so it is normalized to one.

While the first definition focuses on the monomeric units of the polymer chains, the second focuses on empty cells, which allow mobility. Both definitions seem to be similar, but the difference between them can be emphasized by using the simplified bidimensional example shown in Fig. 4. The

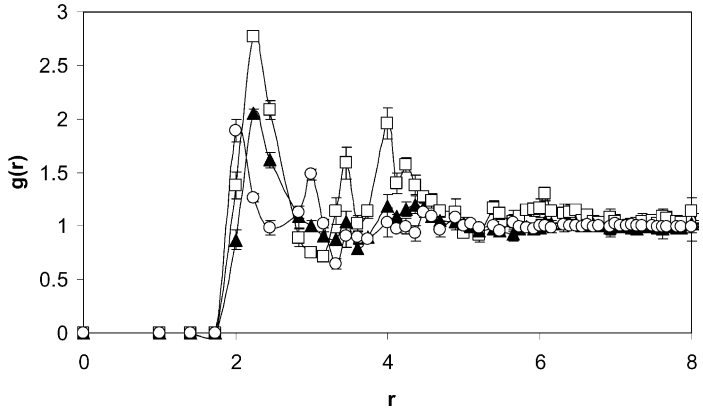


Fig. 2. Pair correlation function as a function of the distance measured in lattice units at temperatures below the transition ($k_BT=0.1$) for $B_f=0$ (□), $B_f=5$ (▲) and $B_f=\infty$ (○). Error bars consisted of ($\pm 3\sigma$) and were sized as dots. Lines are employed only as a guideline for the eye.

application of Wittmann's definition in order to calculate specific volume twice takes into account the two emphasized empty cells (Fig. 4) between monomers (once per monomer). However, if we calculate the DAV, these empty cells, which have to be considered as holes, are considered only once. This second definition seems a more accurate expression of the real mobility of the system, since these cells can be occupied only once, due to the condition concerning volume exclusion. Thus, a better result can be obtained if we focus on the empty cells, which contribute to the system dynamics, as the DAV does.

The original definition of DAV has been employed for athermal systems, so in this paper we calculated DAV considering only kinetic conditions ((i) and (ii) in Wittmann's defitinion), but, as Wittmann pointed out, condition (ii) is governed by temperature, thus its influence must also be taken into account in the DAV. Obviously an extension of the DAV definition employing the Metropolis criterion in thermal systems would give a better performance. This is a task that must be dealt with in the future.

Fig. 5 shows the temperature dependence of DAV during the process described at the beginning of this section. Its evolution is similar to that shown by the energy (Fig. 1). The transitions that appear in the simulations conducted with $B_f=0$ and $B_f=1$ were sharper than those obtained with a combination of inter- and intra-molecular potentials. It is worth noting the significant amount of accessible volume at temperatures below the transition. The value of $\sigma=2.0$ caused the minimum energy configuration to correspond to a configuration with free cells between the monomeric units.

### 3.3. Physical ageing

To characterize quantitatively the evolution of the energy during the isothermal process at temperatures below the transition, the total energy loss during annealing ($10^7$ Monte Carlo steps) is shown in Fig. 6.

Simulations with $B_f \leq 1$ yield a quite well defined long-range order at low temperatures, as explained above. Very small values of the energy loss during isothermal annealing were found in these cases, which further prove that the transition shown in these simulations can be compared to a crystallization process that produces a fully immobile structure. The maximum energy change was obtained within the interval $3 \leq B_f \leq 10$. Concerning the influence of $B_f$ on the physical ageing kinetics, Fig. 7 shows the time

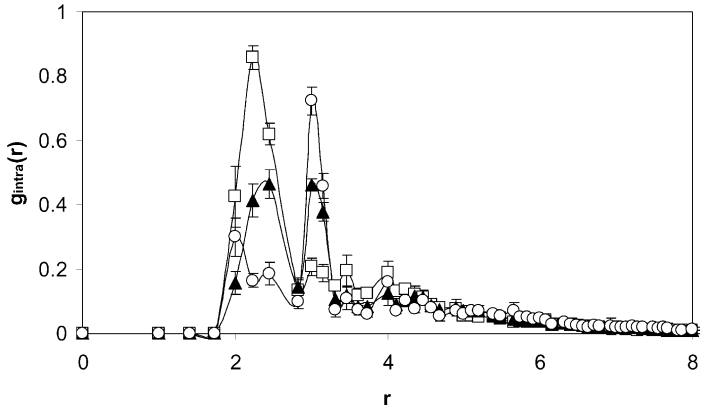


Fig. 3. Intra-molecular contribution to pair correlation function as a function of the distance measured in lattice units at temperatures below the transition ($k_BT=0.1$) for $B_f=0$ (□), $B_f=5$ (▲) and $B_f=\infty$ (○). Error bars consisted of ($\pm 3\sigma$) and were sized as dots. Lines are employed only as a guideline for the eye.

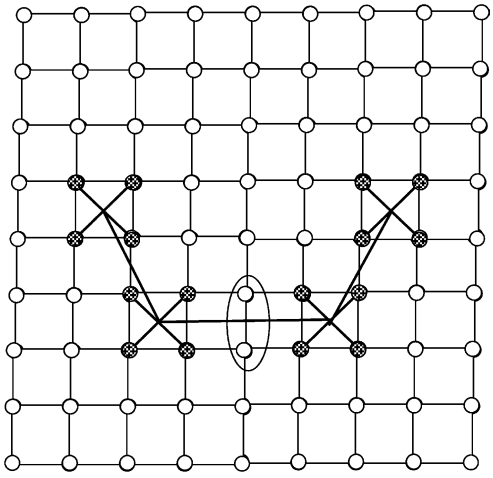

Fig. 4. Schema of four consecutive monomeric units of a polymer chain. The emphasized empty cells are taken into account in different ways, depending on the definition of specific volume. A bidimensional graph is shown in order to simplify the explanation, but a 3D graph can be easily extrapolated. See text.

evolution of the DAV during the isothermal annealing. The change in this accessible volume during isothermal annealing is almost absent, with both $B_f \leq 1$ and $B_f = \infty$. After cooling, at the beginning of the isothermal stage, when only the intra-molecular potential is considered ($B_f = \infty$), the value of DAV is quite high, most of the bonds between polymer segments correspond to the (3,0,0) vector leaving free positions between them, producing the sharp characteristic peak at this distance in the intra-molecular contribution to $g(r)$ shown in Fig. 3. This structure allows easy conformational changes as shown by the evolution of the $g_3(t)$ parameter (Fig. 8) or the high value of the diffusion coefficient $D$ calculated from Fig. 8 at isothermal conditions ($k_BT = 0.1$) (Fig. 6). Nevertheless, this mobility does not

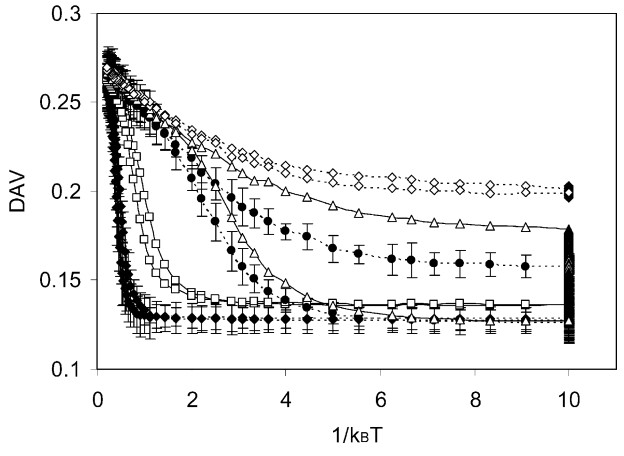


Fig. 5. Evolution of the dynamically accessible volume, DAV, of the system in the process described in the caption to Fig. 1. Simulations conducted with $B_f = 0$ (♦), $B_f = 1$ (□), $B_f = 5$ (●), $B_f = 10$ (△) and $B_f = \infty$ (■). Error bars consisting of ($\pm 3\sigma$) are shown for several data points. The rest are similar to those shown. Lines are drawn only as a guideline for the eye.

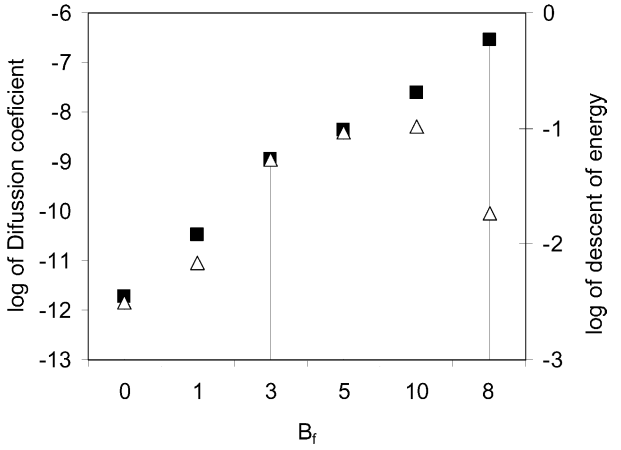


Fig. 6. Diffusion coefficient (■) and energy loss (△) in a period of $10^7$ Monte Carlo steps in an isothermal annealing at $k_BT = 0.1$ in the glassy state.

cause the evolution of either the dynamically accessible volume (Fig. 7) or energy (Fig. 6) towards lower values. From the thermodynamic point of view, the force that causes equilibrium is the excess free energy of the system that makes the polymer chains tends to pack together. The lack of the Lennard–Jones potential makes the model fail in this essential feature of the vitrification of the system. However, when the Lennard–Jones potential predominates, the resulting crystalline structure after cooling contains well packed chains leaving very few free lattice positions available for motion at low temperatures and we cannot compare this to glass transition. Now the $g_3$ parameter shows almost no evolution with time and the diffusion coefficient takes values in the order of magnitude of $10^{-11}$/$10^{-13}$ (lattice length units squared per MCS). Only the combination of both potentials, $3 \leq B_f \leq 10$, yields a spatial distribution of the chains that allows mobility, DAV continuously decreases throughout physical ageing seeking the minimum energy of the system, and it is interesting to

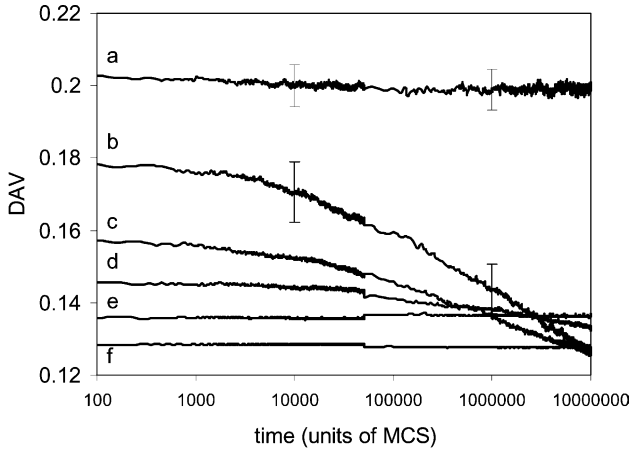


Fig. 7. Dynamically accessible volume evolution during annealing at $k_BT = 0.1$. The simulations were conducted with $B_f = 0$ (f), $B_f = 1$ (e), $B_f = 3$ (d), $B_f = 5$ (c), $B_f = 10$ (b) and $B_f = \infty$ (a). Error bars represent $\pm 3\sigma$.

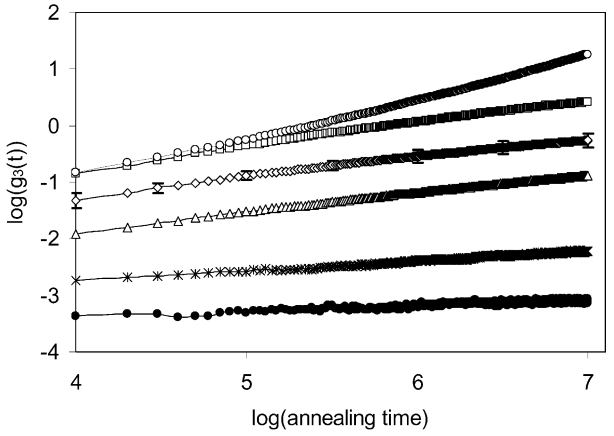


Fig. 8. Function $g_3(t)$ evolution during annealing at constant temperature $k_BT=0.1$ for $B_f=0$ (●), $B_f=1$ (×), $B_f=3$ (△), $B_f=5$ (■), $B_f=10$ (□) and $B_f=\infty$ (○). Only $B_f\geq 3$ shows an appreciable evolution during the simulation time. All error bars ($\pm 3\sigma$) are similar to those shown for $B_f=5$.

note that the DAV finally attained in very long annealing times can go even slightly below the values corresponding to the simulations with $B_f=0$. We can, therefore, conclude that we are observing glass transition only at this intermediate range of $B_f$.

This is already an indication that simulations conducted only with inter-molecular potential or only with intra-molecular potential, yielding quite different transition profiles and different final structures, coincide in failing in the prediction of physical ageing. It is the use of an appropriately balanced combination of both potentials that yields a structure at low temperatures in which conformational motions of polymer chain segments are still possible and produces a continuous molecular packing, as indicated by the numerous experimental results obtained in glass-forming systems.

Experimental results of photon correlation spectroscopy [59] have shown the presence of a long relaxation time tail in the relaxation dynamics of glass-forming materials. This feature could be explained by heterophase fluctuations leading to ultraslow relaxation modes. This concept can be related to the non-ergodicity parameter. The same idea has been advanced from model coupling theory and model simulation [60,61]: two different glasses are formed that differ in their long-term dynamics. The model simulation conducted in this work does not allow to reach a conclusion with respect to the spatial distribution of the dynamically accessible volume. The introduction in the model of a sophisticated characterization of lattice vacancies could inform on the formation of low-mobility clusters during glass formation. In this line, Dawson and his group [62] have recently proposed a characterization of the connectivity of the vacancies.

A series of simulations were conducted with $B_f=5$ and thermal histories that include an isothermal annealing at $k_BT=0.1$ for different annealing times: $10^3$, $10^4$, $10^5$, $10^6$ and $10^7$ MCS. Fig. 9(a) and (b) show the evolution of energy and DAV in the heating scan after the isothermal stage. Both in terms of energy and in DAV, the profile corresponds to that expected from the experiments conducted in glass-forming systems. The lines are more or less parallel while the system is still in the glass state, with smaller values for DAV and energy as the annealing time increases. Subsequently, in the temperature interval in which glass transition takes place, the lines approach the common equilibrium line. For high annealing times, the line corresponding to the heating scan crosses the extrapolation of the equilibrium line and the approach to equilibrium takes place at DAV and energy values smaller than those for equilibrium. This is a characteristic feature of experiments conducted in the dilatometric and calorimetric studies of physical ageing [63,64], and gives rise to the overshoot in the DSC thermograms measured after isothermal annealing and the expansion coefficient in dilatometric experiments. The behavior reproduced by the model is thus qualitatively correct.

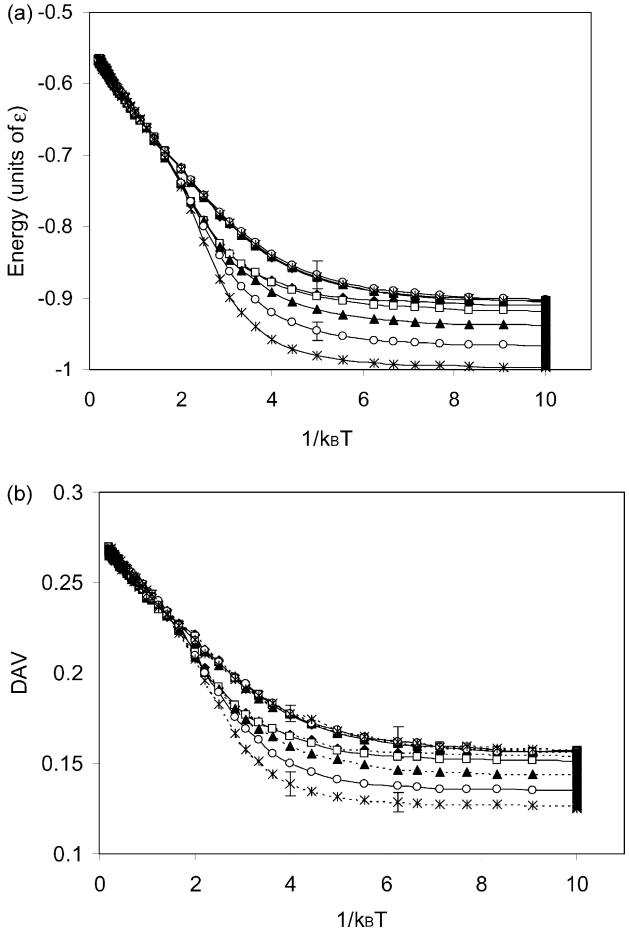


Fig. 9. Energy (a) and dynamically accessible volume (b) evolution of the system during a heating ramp that follows an isothermal annealing at $k_BT=0.1$ for different annealing times: $10^3$ (♦), $10^4$ (□), $10^5$ (▲) and $10^6$ (○) Monte Carlo Steps. The simulations were conducted with $B_f=5$. Error bars representing ($\pm 3\sigma$) are all similar to those shown at several data points.

### 3.4. Dynamically accessible volume at the glass transition temperature

The position of the transition in the temperature axis can be characterized by a glass transition temperature, determined by the onset of the energy or DAV drop in the cooling ramp, as is usual in thermal analysis. The values of $T_g$ obtained from the energy and DAV plots of Figs. 1 and 5 were very similar (Fig. 10).

With the exception of the simulations conducted with $B_f \leq 1$, which can be compared to crystallization, as shown in the previous section, $T_g$ depends only slightly on the value of $B_f$, as shown in Fig. 10.

The dynamically accessible volume is an interesting tool when comparing the influence of the parameters of the simulation on transition behaviour, since its definition implies a normalization that makes the equilibrium lines independent of the energy parameters (Fig. 5). On the other hand, the energy plots do strongly depend on these parameters (Fig. 1).

The dynamically accessible volume has been proposed as a universal parameter to explain glass transition as a lack of mobility. The critical value of the DAV should characterize the onset of glass transition. The different values of $B_f$ can be considered as different glass-forming systems. As shown in Fig. 10, the value of DAV calculated at the onset $T_g$ continuously increases with increasing $B_f$. This is a strong indication that the use of DAV in thermal systems must include the Metropolis criterion. A step in this direction would be to consider the contribution of an empty cell to the dynamic accessible volume as the probability of being occupied in a single move, according to Eq. (3). As an example of the role of temperature in the DAV calculation we can consider the case of $B_f = \infty$ (bond length potential only). At low temperatures, below the transition, one of the preferred final configurations is that of bond vectors (3,0,0) in which the distance between consecutive monomeric units is three lattice units (Fig. 3). The two free cells between monomeric units in the middle of the chain are not considered as DAV, since the maximum bond length must be exceeded in order to occupy them. However, this is not the case of the chain ends represented in the schema of Fig. 11. The emphasized empty cells can be occupied in athermal conditions, although the Metropolis criterion would give a low probability of that motion. Four of such cells per chain in the bidimensional model and eight in the 3D lattice are in this situation. These empty cells can account for up to 5% of the lattice and are considered to be DAV in athermal calculations, although they make no contribution to the mobility of the system. As the chain length increases, this effect becomes less important, thus the maximum excess DAV would be 2.5% if $N=20$ and 1.675% if $N=30$. When we have two energies the increase in DAV is less, since there are fewer bond vectors in the (3,0,0) position (Fig. 3).

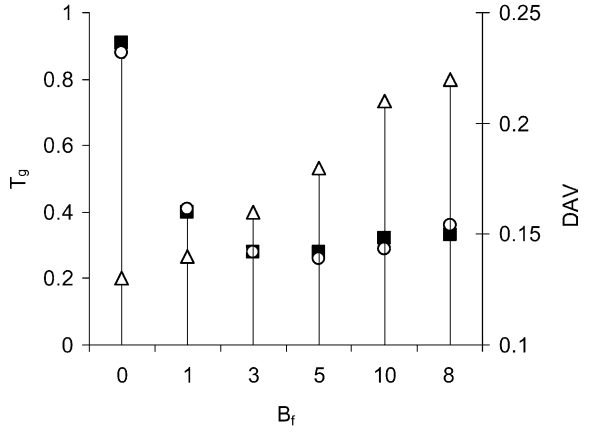


Fig. 10. Glass transition temperature (onset of the glass transition, see text) determined from the temperature dependence of energy (■) and DAV (○). The value of DAV at $T_g$ onset is also represented (△).

In order to further quantify this effect, the simulation of a process with the same thermal history as that which produced the results shown in Fig. 5 was repeated with two systems with $N=20$ and $N=30$ for $B_f = \infty$. The rest of the simulation parameters were kept unaltered. Both systems showed a similar observed $T_g$ onset and DAV at this temperature, which was around 1% lower than in the system with $N=10$.

Consequently, at least a part of the increase in the value of DAV at the onset of the transition with increasing $B_f$ can be explained by the artefact described in the preceding paragraphs, but other contributions cannot be ruled out. It can be said that the dynamically accessible volume can be considered a good parameter for observing glass transition, showing a decrease as temperature decreases, although the critical DAV value that indicates the beginning of the

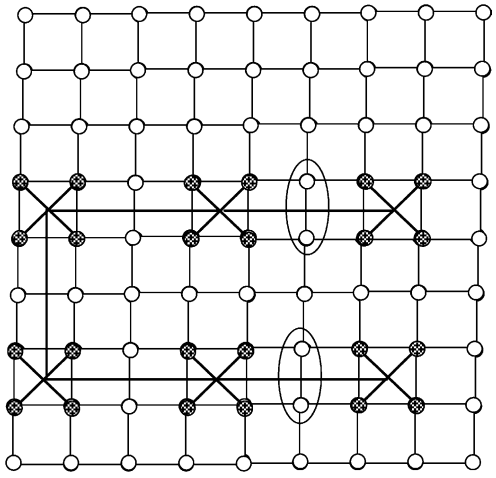

Fig. 11. Schema showing a polymer chain consisting of six consecutive monomeric units in a bidimensional simulation. Emphasized cells in an external bond are considered as dynamically accessible volume when bond vector is (3,0,0) but these cells are not accessible at temperatures below the glass transition due to Metropolis criterion. A bidimensional graph is shown in order to simplify the explanation, but a 3D graph can be easily extrapolated.

transition could depend on the characteristics of the system. Further work is necessary to determine whether a modification of the definition of the dynamically accessible volume could yield a universal parameter that characterizes glass transition in thermal systems.

## 4. Conclusions

The collapse of molecular mobility that causes glass transition when a polymer melt is cooled from a state of equilibrium is due to various physical features such as chain connectivity, inter-molecular interaction potentials, chain stiffness and geometrical restrictions to the diffusion of the chain segments, among others. Computer simulation based on Monte Carlo calculations can help in understanding the role of each of these aspects in the complex vitrification phenomenon.

There are two key experimental characteristics of glass transition: the change in the temperature dependence of the energy and specific volume in a more or less narrow temperature interval, and the non-equilibrium character of the glass state shown by the structural relaxation or physical ageing process. The bond fluctuation model shows that the model prediction of these two features requires the consideration of both inter- and intra-molecular interaction potentials. The balance between the forces of these two contributions to the energy of the system determines the residual mobility of the chain segments in the glass state and is the driving force that guides the evolution of the system towards thermodynamic equilibrium at temperatures below glass transition.

The dynamically accessible volume is a very useful variable to characterize the vitrification process and the segmental dynamics in the glass state. It has been shown that the dynamically accessible volume at the onset of glass transition may depend on the characteristics of the system. This suggests that the definition of the accessibility of an empty cell in the framework of the Bond fluctuation model in thermal systems must in some way involve the Metropolis criterion.

## Acknowledgements

The authors are grateful for the support given by the Spanish Science and Technology Ministry through the MAT2003-05391-C03-01 project. We would like to thank the R + D + i Linguistic Assistance Office at the Universidad Politecnica of Valencia for their help in revising this paper.

## References

[1] Johary GP, Hallbrucker A, Mayer E. Nature 1987;330:552.
[2] Davies RO, Jones GO. Adv Phys 1953;2:370.
[3] Metropolis N, Rosenbluth AW, Rosenbluth MN, Teller AH, Teller E. J Chem Phys 1953;21:1087–92.
[4] Bennemann C, Baschnagel J, Paul W. European Phys J B 1999;10: 323.
[5] Bennemann C, Baschnagel J, Paul W, Binder K. Comput Theor Polym Sci 1999;9:217.
[6] Moe N, Ediger MD. Phys Rev E 1999;59(1):623–30.
[7] Dünweg B, Kremer K. Phys Rev Lett 1991;66(23):2996–9.
[8] Kremer K, Grest GS, Carmesin I. Phys Rev Lett 1988;61(5):566–9.
[9] Naess SN, Adland HM, Mikkelsen A, Elgsaeter A. Physica A 2001; 294:323–39.
[10] Fukui K, Sumpter B, Barnes M, Noid D. Polym J 1999;31(8):664–71.
[11] Kenkare NR, Hall CK, Khan A. J Chem Phys 2000;113(1):404–18.
[12] Duering ER, Kremer K, Grest GS. Phys Rev Lett 1991;67(25): 3531–4.
[13] Neelov I, Darinskii A, Balabaev N, Sundholm F. Polym Sci 1998; 40(12):1203–11.
[14] Liu H, Chakrabarti A. Polymer 1999;40:7285–93.
[15] Bennemann C, Paul W, Baschnagel J, Binder K. J Phys: Condens Matter 1999;11:2179.
[16] Alder BJ, Wainwright TE. J Chem Phys 1957;27(5):1208–9.
[17] Binder K. Monte Carlo and molecular dynamics simulations in polymer science. Oxford: Oxford University Press; 1995.
[18] Kremer K, Lyklema JW. Phys Rev Lett 1985;54(4):267–9.
[19] Vanderzande C. Lattice models of polymers. Cambridge: Cambridge University Press; 1998.
[20] Balogh MP, Madden WG. Macromolecules 1997;30:5096–103.
[21] Lobe B, Baschnagel J, Binder K. Macromolecules 1994;27:3658–65.
[22] Toma L, Toma S, Subirana J. Macromolecules 1998;31:2328–34.
[23] Clancy TC, Webber SE. Macromolecules 1997;30:1340–6.
[24] Müller M, Binder K. Macromolecules 1998;31:8323–46.
[25] Lai PY. Chin J Phys 1998;36(3):494–500.
[26] Okun K, Wolfgardt M, Baschnagel J, Binder K. Macromolecules 1997;30:2075–3085.
[27] Binder K. Comput Phys Commun 1999;121:168–75.
[28] Baschnagel J. J Phys: Condens Matter 1996;8:9599–603.
[29] Paul W. In: Proceedings of the international workshop on non equilibrium phenomena in supercooled fluids, glasses and amorphous materials, 1996. p. 220–4.
[30] Wittkop M, Hölzl T, Kreitmeier S, Göritz D. J Non-Cryst Solids 1996; 201:199–210.
[31] Tanaka M, Iwata K, Kuzuu N. Comput Theor Polym Sci 2000;10: 299–308.
[32] Carmesin I, Kremer K. Macromolecules 1988;21:2819–23.
[33] Deutsch H, Binder K. J Chem Phys 1990;94:2294–304.
[34] Paul W, Binder K, Heermann D, Kremer K. J Chem Phys 1991; 95(10):7726–40.
[35] Wittmer J, Paul W, Binder K. Macromolecules 1992;25:7211–9.
[36] López Rodriguez A, Wittmann HP, Binder K. Macromolecules 1990; 23:4327–35.
[37] Yong CW, Higgs PG. Macromolecules 1999;32:5062–71.
[38] Muller M, Binder K, Schäfer L. Macromolecules 2000;33:4568–80.
[39] Rubio A, Storey M, Felicity J, Lodge M, Freire JJ. Macromol Theory Simul 2002;11(2):171–83.
[40] Muller M. Macromolecules 1997;30:6353–7.
[41] Baschnagel J, Paul W, Tries V, Binder K. Macromolecules 1998;31: 3856–67.
[42] Deutsch HP, Binder K. Macromolecules 1992;25:6214–30.
[43] Müller M. Macromolecules 1995;28:6556–64.
[44] Müller M, Binder K. Macromolecules 1995;28:1825–34.
[45] Jilge W, Carmesin I, Kremer K, Binder K. Macromolecules 1990;23: 5001–13.
[46] Scot Shaffer J. Macromolecules 1996;29:1010–3.
[47] Trautenberg HL, Hözl T, Göritz D. Comput Theor Polym Sci 1996;6: 135–41.
[48] Baschnagel J, Binder K. Physica A 1994;204:47–75.

[49] Baschnagel J, Binder K, Doruker P, Gusev A, Hahn O, Kremer K, et al. Adv Polym Sci 2000;152:44–156.
[50] Tries V, Paul W, Baschnagel J, Binder K. J Chem Phys 1997;106(2): 738–48.
[51] Sadus R. Molecular simulation of fluids. Theory, algorithms and object-orientation. Amsterdam: Elsevier; 1999.
[52] Binder K, Paul W. J Polym Sci, Part B: Polym Phys 1997;35:1–31.
[53] Starr FW, Sastry S, Douglas JF, Glotzer SC. Phys Rev Lett 2002;89: 125501.
[54] Wittmann HP, Kremer K, Binder K. J Chem Phys 1992;96: 6291–306.
[55] Wolfgardt M, Baschnagel J, Paul W, Binder K. Phys Rev E 1996; 54(2):1535–43.
[56] Dawson KA, Lawlor A, McCullagh GD, Zaccarelli E, Tartaglia P. Physica A 2002;316:115–34.
[57] Dawson KA, Lawlor A, DeGregorio P, McCullagh GD, Zaccarelli E, Fo G, et al. Faraday Discuss 2003;123:13–26.
[58] Lawlor A, Reagan D, McCullagh GD, De Gregorio P, Tartaglia P, Dawson K. Phys Rev Lett 2002;89(24):245503.
[59] Fischer EW, Bakai A, Patkowski A, Steffen W, Reinhardt L. J Non-Cryst Solids 2002;307–310:584.
[60] Zaccarelli E, Foffi G, Dawson KA, Buldyrev V, Sciortino F, Tartaglia P. Phys Rev E 2002;66:041402.
[61] Zaccarelli E, Foffi G, Dawson KA, Buldyrev V, Sciortino F, Tartaglia P. J Phys: Condens Matter 2003;15:S367.
[62] Lawlor A, De Gregorio P, Dawson KA. J Phys: Condens Matter 2004; 16:S4841.
[63] Kovacs AJ, Aklonis JJ, Hutchinson JM, Ramos AR. J Polym Sci, Polym Phys Ed 1979;17:1097.
[64] Hodge IM. J Non-Cryst Solids 1994;169:211.